Available online at www.sciencedirect.com

ScienceDirect

Journal of Nuclear Materials 375 (2008) 213–217

journal of nuclear materials

www.elsevier.com/locate/jnucmat

Heat load behaviors of plasma sprayed tungsten coatings on copper alloys with different compliant layers

F.L. Chong [a,*], J.L. Chen [a], J.G. Li [a], D.Y. Hu [b], X.B. Zheng [b]

[a] Institute of Plasma Physics, Chinese Academy of Sciences, Hefei 230031, China

[b] Shanghai Institute of Ceramics, Chinese Academy of Sciences, Shanghai 200051, China

Received 5 October 2007; accepted 23 November 2007

Abstract

Plasma sprayed tungsten (PS-W) coatings with the compliant layers of titanium (Ti), nickel–chromium–aluminum (NiCrAl) alloys and W/Cu mixtures were fabricated on copper alloys, and their properties of the porosity, oxygen content, thermal conductivity and bonding strength were measured. High heat flux tests of actively cooled W coatings were performed by means of an electron beam facility. The results indicated that APS-W coating showed a poorer heat transfer capability and thermo-mechanical properties than VPS-W coating, and the compliant layers improved W coating performance under the heat flux load. Among three compliant layers, W/Cu was the preferable because of its better effects on heat removal and stress alleviating. The optimization of W/Cu compliant layer found that 0.1 mm and 25 vol.%W was optimum compliant layer structure for 1 mm W coating, which induced a 23% reduction of the maximum stress compared to the sharp interface, and the plastic strain was reduced to 0.01% from 1.55%.

PACS: 52.40.Hf; 81.05.Bx; 81.15.−z

1. Introduction

Tungsten (W) seems a promising plasma facing material (PFM) due to its low sputtering erosion yield and prominent thermal–mechanical properties [1–3]. But in order to overcome its disadvantages of the heavy weight and poor workability [4], plasma spraying technology is considered a good integration way of armor material to heat sink, which offers the ability to coat large area, even complex shapes and in situ repair of damaged parts [5]. Plasma sprayed tungsten (PS-W) coatings on carbon based materials have been successfully fabricated [6,7], and preliminary experimental databases about PS-W coating application as PFM were obtained from the plasma campaign of ASDEX Upgrade [8,9] and TEXTOR [10,11] tokamaks. But tungsten coating deposited on the copper–chromium–zirconium (CuCrZr) alloys is a challenge due to the larger mismatch of their thermal expansion coefficients (CTE) and Young's modulus, which will induce the stress concentration on the interface of plasma facing component (PFC) and degrade the bonding property of W coating on CuCrZr substrate. So to overcome these matters, the application of the compliant layer is necessary, which must have an intermediate thermal expansion coefficient and high compliance [12].

In the paper, PS-W coatings and their properties were introduced, and titanium (Ti), nickel–chromium–aluminum (NiCrAl) alloys and W/Cu mixtures were used as compliant layers to analyze the thermal performance under the heat flux, which is also estimated by ANSYS code. Finally, the thickness and W/Cu composition ratios of W/Cu compliant layer were optimized.

2. PS-W coatings on CuCrZr

The spraying campaign was carried out using a F4-torch by means of the plasma spraying facility manufactured by Sulzer-Metco, Switzerland. Tungsten powder with an

* Corresponding author. Fax: +86 551 5591310.
E-mail address: flch@ipp.ac.cn (F.L. Chong).

0022-3115/$ - see front matter © 2008 Elsevier B.V. All rights reserved.
doi:10.1016/j.jnucmat.2007.11.008

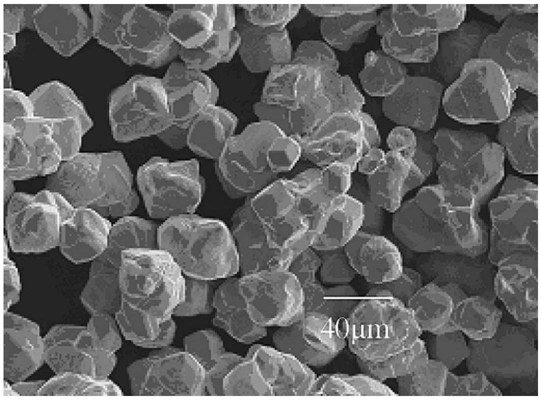

Fig. 1. SEM image of W powder.

average size of 40 μm shown in Fig. 1 was applied to spray W coating. In order to strengthen the adhesion of the coating with the substrate, pretreatment of the substrate including grit blasting, ultra-sonic cleaning and argon plasma sputter cleaning was made before the plasma spraying campaign. W/Cu mixtures have the flexible ratios of W to Cu, and the thermal expansion coefficients and the Young's modulus are between that of W and CuCrZr, so W/Cu was used as one of the candidate compliant layers. Ti is also chosen as a kind of compliant layer at present due to its light weight, another candidate compliant layer is NiCrAl. As a comparison, the coating with the sharp interface was also fabricated.

One millimeter W coatings were fabricated by means of two kinds of methods: vacuum plasma sprayed W (VPS-W) coatings and air plasma sprayed W (APS-W) coatings. The main properties of W coatings are listed in Table 1, and the properties of VPS-W coatings are supposed to be the same with each other, because they were be fabricated under the same parameters. Fig. 2 shows their distributions of pore size diameter and the porosity, which were measured by means of mercury porosimeter instrument (AutoPore IV 9500) at RT. The low porosity of 7.6% and the narrow pore size distribution of 0.08–1 μm were obtained in the VPS-W coating, however, in the APS-W coating, it was 12.9% and the pore size distribution of about 100 μm was observed except the pore of 0.08–1 μm, which was also the main reason why APS-W coating had much more pores than VPS-W coating. The oxygen content of the VPS-W coating was measured to about 0.35 wt% by means of the energy dispersive spectroscope (EDS), and that of APS-W reached 1.2 wt%. The thermal conductivities of W coatings were measured by means of laser flash method at RT, which shows the 59.3 W/mK for VPS-W coating, however, for APS-W coating, it was only 32.3 W/mK. May be the differences of the oxygen content and porosity can well explain the large differences of the thermal conductivities between both coatings. The bonding strengths of W coatings were carried out according to ASTM C-633-79 standard by the tensile tests. VPS-W coating with the W/Cu compliant layer has the maximum bonding strength of 44.8 MPa, and it is 34.5 MPa for the sharp interface W coating. W coatings with the Ti and NiCrAl compliant layers have the similar bonding strength of about 22 MPa with the APS-W coating. Analysis of failure surface showed that the bonding strength at the interface of compliant layer and CuCrZr was poor, where the failure was easy to occur.

Table 1
The main properties of W coatings

Spraying method	Compliant layer	Porosity (%)	Oxygen content (wt%)	Thermal conductivity (W/mK)	Bonding strength (MPa)
APS-W	W/Cu	12.9	1.2	32.3	22.7
VPS-W	W/Cu	7.6	0.35	59.3	44.8
	Ti	–	–	–	21.0
	NiCrAl	–	–	–	22.6
	No	–	–	–	34.5

3. Heat flux tests of W coatings

Heat load tests were carried out in the electron beam facility at ASIPP under the vacuum of 1.5–4 × 10^{-3} Pa. The heat flux was loaded on an area of 20 × 20 mm^2 and increased from 2.5 to 10 MW/m^2 with a step of 1.25 MW/m^2 and each step lasted for about 150 s. Surface temperature was measured by an infrared pyrometer

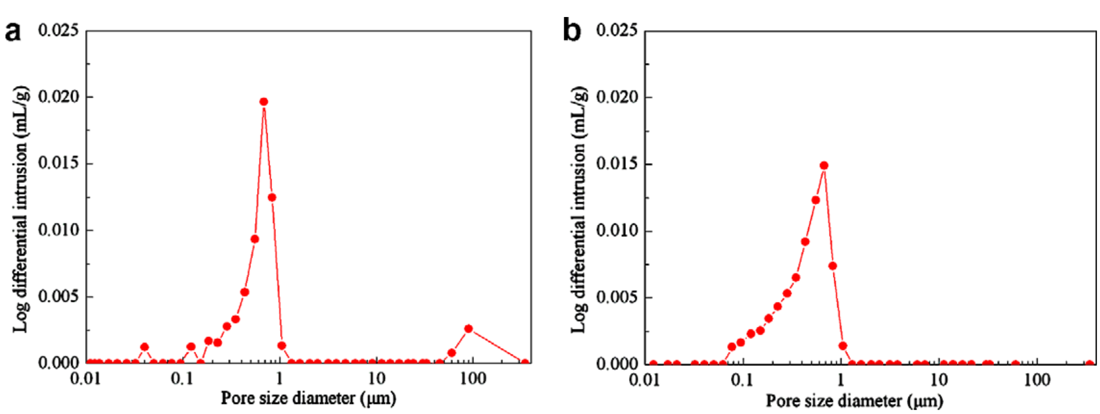

Fig. 2. The distribution of pore size diameter and the porosity. (a) APS-W coating, and (b) VPS-W coating.

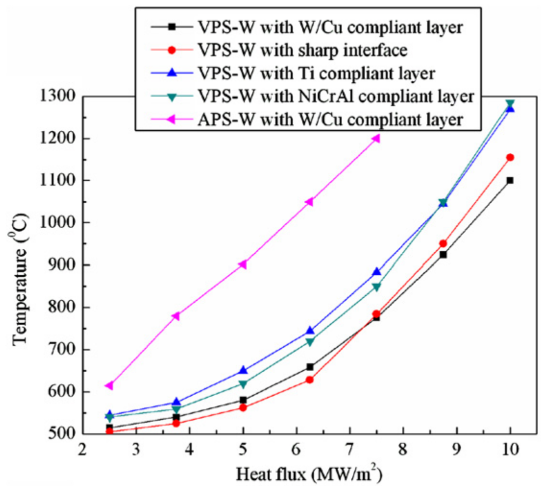

Fig. 3. The surface temperature evolution with the increase of the absorbed power density from 2.5 to 10 MW/m^2.

(500–2000 °C). A water tube of 10 mm diameter was drilled through the center of the heat sink of $24 \times 30\ mm^2$. The water velocity was about 10 m/s, and inlet temperature was 20 °C.

Fig. 3 shows the surface temperature evolution with the increase of the absorbed power density from 2.5 to 10 MW/m^2. It can be seen that at 7.5 MW/m^2 the surface temperature of VPS-W coating with the sharp interface showed the rapid increase, and at the higher heat flux it even exceeded that of VPS-W coating with W/Cu compliant layer. Maybe it was the sign of crack appearing. W coating with the W/Cu compliant layer kept the lower temperature, which was about 1100 °C at 10 MW/m^2. Comparison with W/Cu mixtures, Ti and NiCrAl materials have the lower thermal conductivity, which induced about 150 °C higher surface temperature at 10 MW/m^2. APS-W coating showed the higher surface temperature than VPS-W coating under the same heat flux load due to its poorer heat transfer capability, and it reached 1200 °C at 7.5 MW/m^2.

Surface morphologies of W coatings after the heat flux tests are shown in Fig. 4. Micro-cracks appeared on the surface of APS-W coating. VPS-W coating with the sharp interface also showed the cracks though it kept the lower surface temperature. It also explains the reason why the surface temperature increased after 6 MW/m^2 heat flux. But no cracks were observed on the other VPS-W coatings. The behavior is attributed to the stress alleviating effect of the compliant layer. From the cross sectional SEM images observation, no damages formed.

4. Numerical simulation by ANSYS code

The ANSYS finite element code is used for the present thermal analysis. The temperature dependence of material properties was taken into account, and the rule of mixtures was used to estimate the mechanical properties of W/Cu compliant layer [12,13]. A straight tube with a water velocity of 10 m/s, an inlet pressure of 1 MPa and an average temperature of 50 °C was assumed. The steady state heat flux of 5 MW/m^2 was loaded on the top surface of mock up.

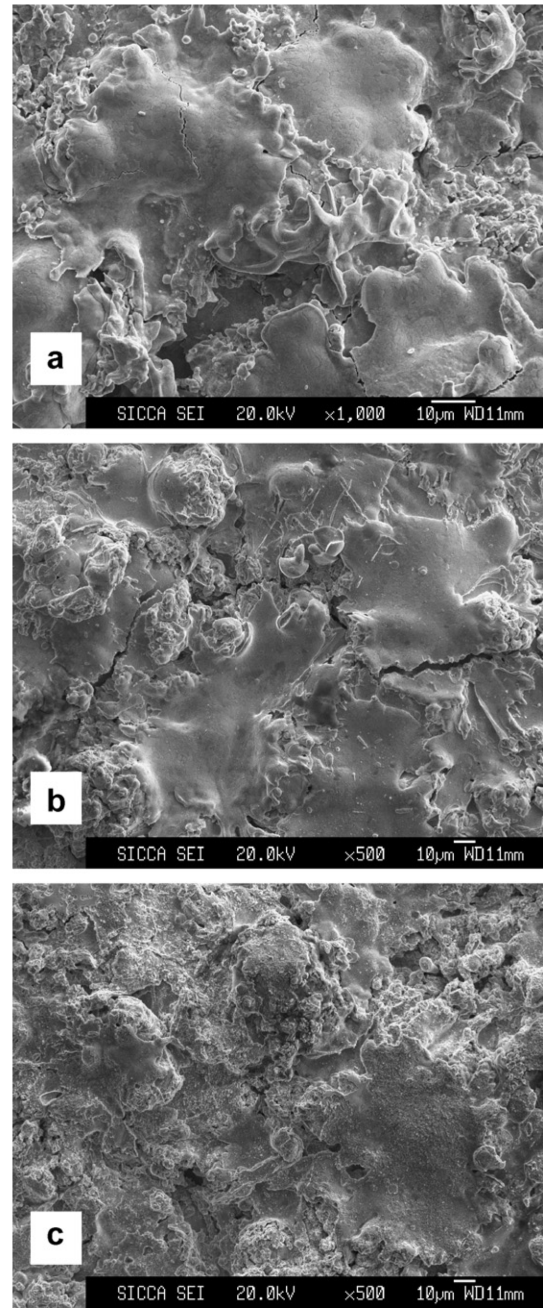

Fig. 4. Surface morphologies of W coatings after the heat flux tests. (a) APS-W, (b) VPS-W with the sharp interface, and (c) VPS-W with W/Cu compliant layer.

4.1. Choice of compliant layers

The surface temperatures of W coatings with 0.5 mm compliant layers under the heat flux of 5 MW/m^2 are shown in Fig. 5. The surface temperatures increased due to inserting the compliant layers, and the increment

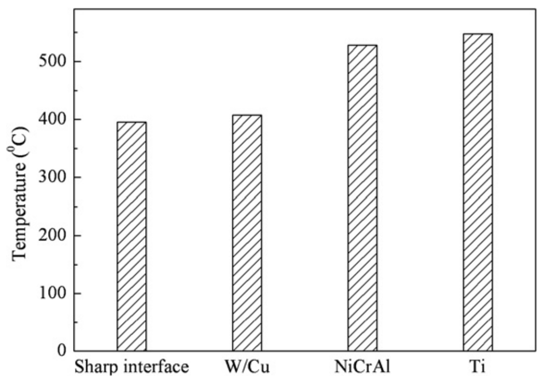

Fig. 5. The surface temperatures of W coatings with 0.5 mm compliant layers under the heat flux of 5 MW/m^2.

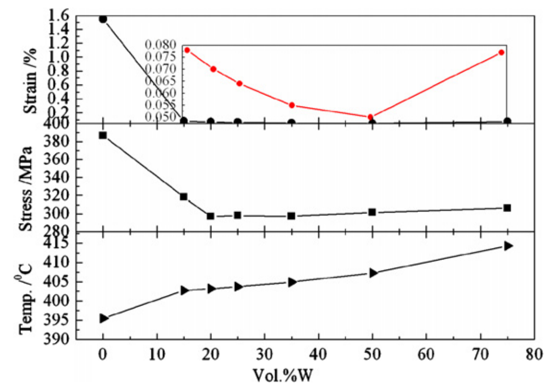

Fig. 7. The surface temperature, Mises stress, and plastic strain versus W volume fraction in 0.5 mm W/Cu compliant layer.

depended on the thermal conductivity of the compliant layers. Ti and NiCrAl, which have the lower thermal conductivity, made the surface temperature increase to the 547.5 °C, however, only 11.8 °C were increased when W/Cu was used.

A comparison of 3-D Mises stresses for the different compliant layers under the heat flux of 5 MW/m^2 is shown in Fig. 6. The maximum stress occurred in the interface of compliant layer and heat sink except NiCrAl, where it was adjacent to NiCrAl compliant layer because the mismatch of Young's modulus between W coating and NiCrAl was larger than that between CuCrZr and NiCrAl. The stress was reduced from the 386.6 of the sharp interface coating to about 300 MPa when the compliant layer was applied. The maximum reduction was obtained using W/Cu compliant layer with a 23% reduction compared to the sharp interface. Therefore, it seems that W/Cu was the preferable compliant layer among the candidates of Ti, NiCrAl and W/Cu.

4.2. Optimization of W/Cu compliant layer

Fig. 7 shows the surface temperature, Mises stress, and plastic strain versus W volume fraction (vol.%W) in 0.5 mm W/Cu compliant layer. It can be seen that the stress reduced to the minimum magnitude of 297 MPa from 386.6 MPa when the volume fraction increased to 20%. And the stress slightly increased to 306.4 MPa at 75 vol.%W. The plastic strain was also localized to compliant layer regions adjacent to W coating due to the maximum stress existence. In contrast to the sharp interface, W/Cu compliant layer resulted in the significant plastic strain reduction, though it was already very small (1.55%) for the sharp interface structure. With the increase of volume fraction of W, the plastic strain firstly decreased, and then increased slowly when the composition was beyond 50 vol.%W. The increase of surface temperature was very slowly with the increase of volume fraction of W.

To optimize the thickness of W/Cu compliant layer, the volume fraction of the optimal composition ratios of 25 vol.%W was used. The surface temperature, Mises stress, and plastic strain versus 25 vol.%W compliant layer thickness are shown in Fig. 8. The Mises stress rapidly reduced to 299.1 MPa at 0.1 mm from 386.6 MPa of the sharp interface coating. Then no remarkable change was observed though it increased to 1 mm. The plastic strain evolution with the increase of W/Cu thickness was similar with the stress, which reduced to the magnitude of 0.01% at 0.1 mm. The surface temperature increased slightly with the increase of compliant layer thickness. Further analysis

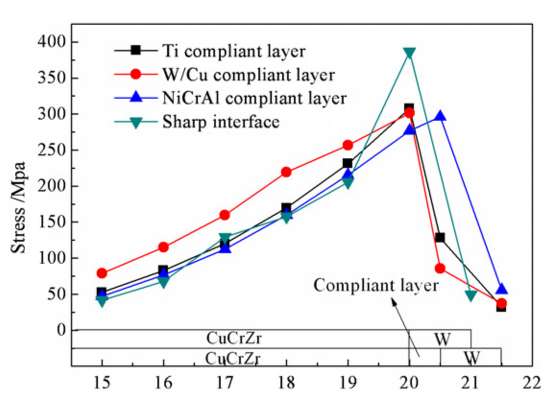

Fig. 6. A comparison of 3-D Mises stresses for the different compliant layers under the heat flux of 5 MW/m^2.

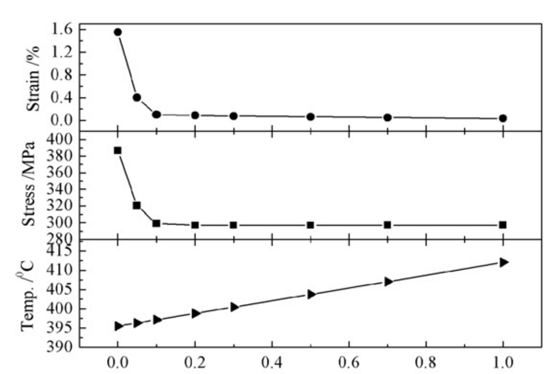

Fig. 8. The surface temperature, Mises stress, and plastic strain versus 25 vol.%W compliant layer thickness.

found that even when the compliant layer is 5 mm thick, the stress only decreased to 282.3 MPa, and mainly caused an increase of surface temperature.

Taking three aspects of the stress, strain and surface temperature into accounts, it can be concluded that 0.1 mm and 25 vol.%W should be optimum compliant layer structure for 1 mm W coating.

5. Conclusion

Plasma sprayed tungsten coatings with the compliant layers of Ti, NiCrAl and W/Cu were fabricated on copper alloys. APS-W coating showed the poorer heat transfer capability and thermo-mechanical properties than VPS-W, which were likely caused by its higher oxygen content and porosity. The compliant layers improved W coatings performance under the heat flux load though the surface temperature was a litter higher than for a W coating with a sharp interface. W/Cu was preferable among three candidate compliant layers considering the heat transfer capability and the effect of alleviating thermal stress. In addition, finite element analysis also found that W/Cu compliant layer of 0.1 mm and 25 vol.%W was optimum for 1 mm W coating, which induced a 23% reduction of the maximum stress compared to the sharp interface, and the plastic strain was reduced to 0.01% from 1.55%.

Acknowledgement

The work was supported by National Natural Science Foundation of China under the Project No. 10475080.

References

[1] N. Yoshida, J. Nucl. Mater. 266–269 (1999) 197.
[2] D. Naujoks, K. Asmussen, M. Bessenrodt-Weberpals, et al., Nucl. Fus. 36 (1996) 671.
[3] R. Dux, V. Bobkov, N. Fedorczak, et al., J. Nucl. Mater. 363 (2007) 112.
[4] K. Tokunaga, N. Yoshida, Y. Kubota, et al., Fus. Eng. Des. 49–50 (2000) 371.
[5] J. Matejicek, Y. Koza, V. Weinzettl, Fus Eng. Des. 77–79 (2005) 395.
[6] S. Deschka, C. Garcia-Rosales, W. Hohenauer, et al., J. Nucl. Mater. 233–237 (1996) 645.
[7] N. Tokunaga, N. Yoshida, K. Noda, et al., J. Nucl. Mater. 258–263 (1998) 998.
[8] K. Krieger, H. Maier, R. Neu, et al., J. Nucl. Mater. 266–269 (1999) 207.
[9] R. Neu, V. Bobkov, R. Dux, et al., J. Nucl. Mater. 363–365 (2007) 52.
[10] T. Tanabe, M. Wada, T. Ohgo, et al., J. Nucl. Mater. 283–287 (2000) 1128.
[11] A. Pospieszczyk, T. Tanabe, V. Philipps, et al., J. Nucl. Mater. 290–293 (2001) 947.
[12] ITER Materials Assessment Report, ITER Document No. G 74 MA 10 01–10-11 W 0.2, 2001.
[13] J. Chapa, I. Reimanis, J. Nucl. Mater. 303 (2002) 131.